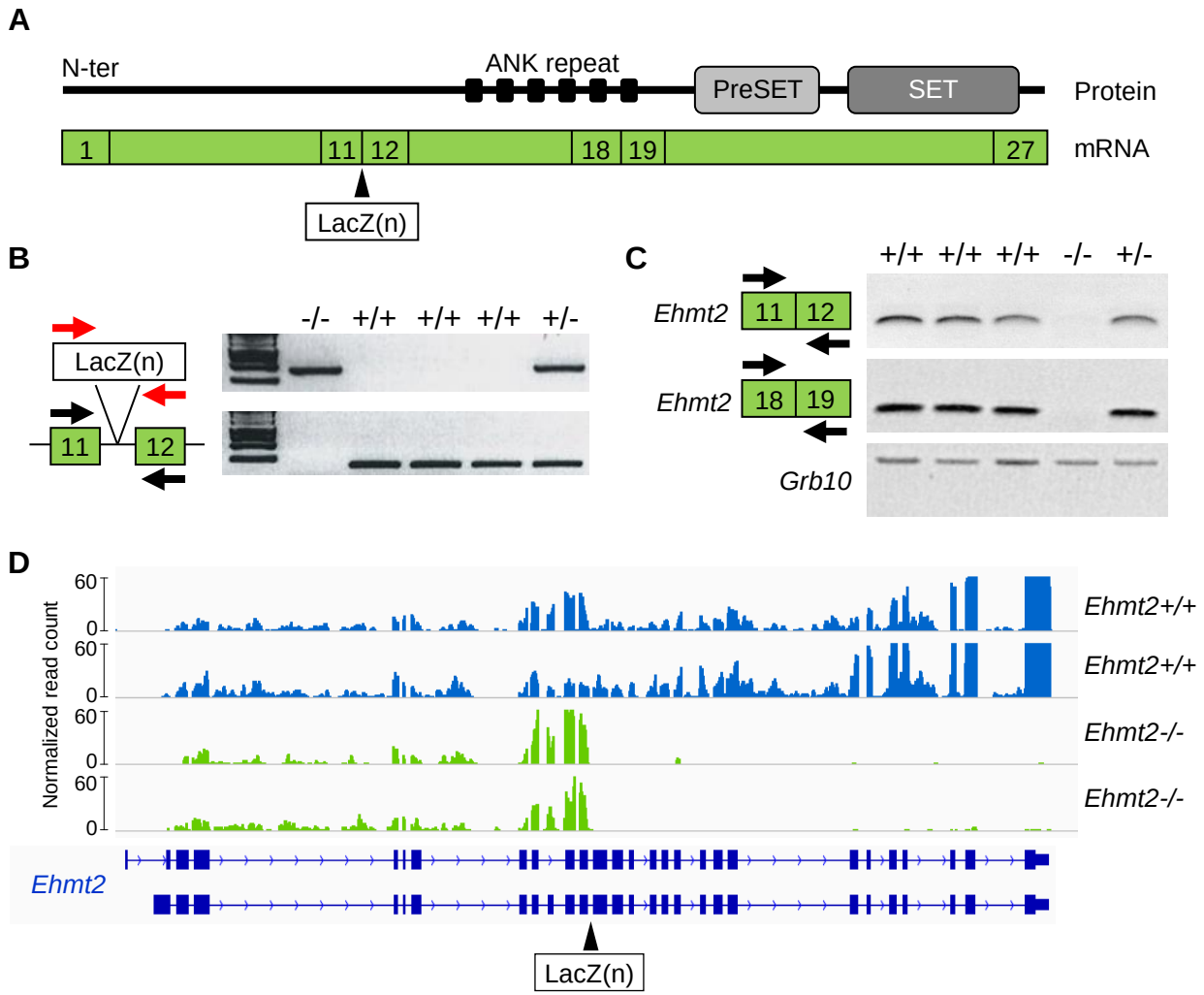

Supplemental Figure S1. Characterization of *Ehmt2*-knockout embryos. A. Schematic representation of the mouse EHMT2 protein (top) and transcript (bottom) with the site of gene trap insertion between the exons 11 and 12 (Wagschal et al., 2008). **B.** Examples of PCR genotyping using two primer pairs in the LacZ insertion cassette (red arrows) and in the exons 11-12 spanning the site of insertion (black arrows). **C.** Expression analysis by RT-PCR with primers spanning exons 11-12 and exons 18-19 (black arrows) indicates that the transcription of the *Ehmt2* gene is abolished after the site of LacZ insertion in *Ehmt2-/-* animals. *Grb10* was amplified as a control. **D.** RNA-seq in E8.5 embryos confirm that the transcription of the *Ehmt2* gene is abolished after the site of LacZ insertion in knock-out embryos.

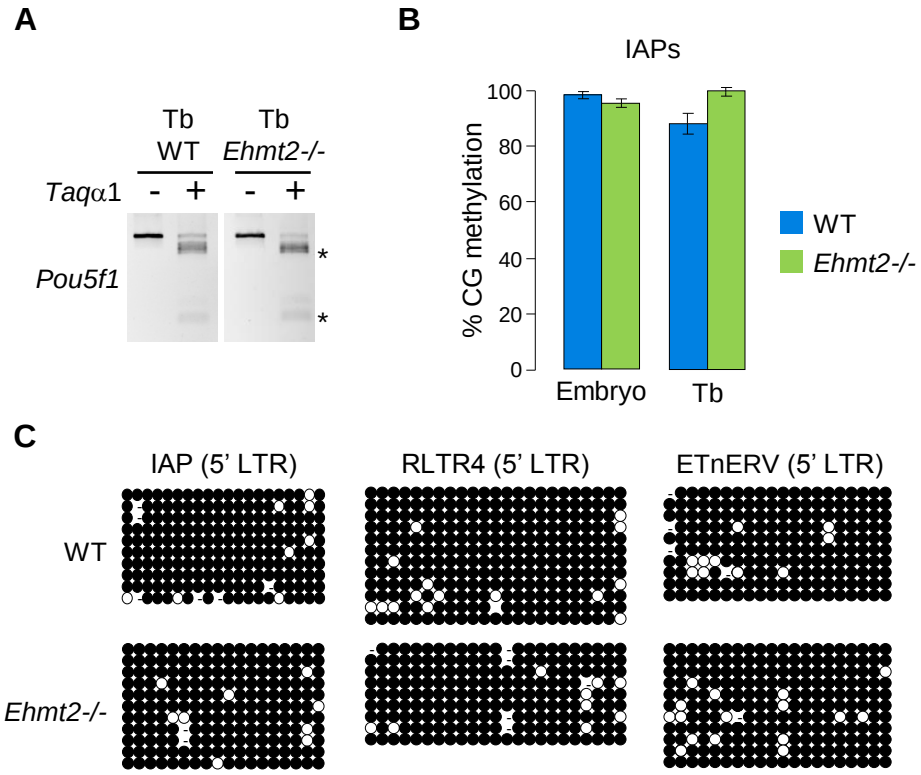

Supplemental Figure S2. Methylation analysis in *Ehmt2-/-* embryos and extra-embryonic tissues. A. COBRA showing that the *Pou5f1* promoter is methylated at similar levels in trophoblast (Tb) cells from WT and *Ehmt2-/-* E9.5 conceptus. **B.** Quantification of DNA methylation in IAP retrotransposons by *Mcr*BC digestion followed by qPCR in WT and *Ehmt2-/-* E9.5 embryos and trophoblast (Tb) (mean ± SD, n=3). **C.** Bisulfite cloning and sequencing at three retrotransposons in WT and *Ehmt2-/-* E9.5 embryos. Circles represent methylated (black) and unmethylated (white) CpGs, small lines indicate undefined methylation status, empty spaces indicate a deleted cytosine. Each horizontal row represents one sequenced clone.

A

Sample	Paired-end reads	Mapping efficiency (%)	Reads with unique hits (%)	Conversion rate (%)	Sequencing depth (median)	CpGs 8x
WT #1	32 547 365	93.98	75.24	99.67	62x	1 313 494
WT #2	47 789 978	93.21	74.44	99.76	91x	1 299 216
WT #3	39 181 062	94.31	75.92	99.78	79x	1 379 871
WT #4	43 058 637	88.20	70.08	99.58	67x	1 365 044
Ehmt2 KO #1	24 574 882	93.09	74.89	99.65	45x	1 336 445
Ehmt2 KO #2	30 063 968	91.56	74.35	99.81	57x	1 224 131
Ehmt2 KO #3	23 032 908	90.40	72.88	99.71	44x	1 243 754

B

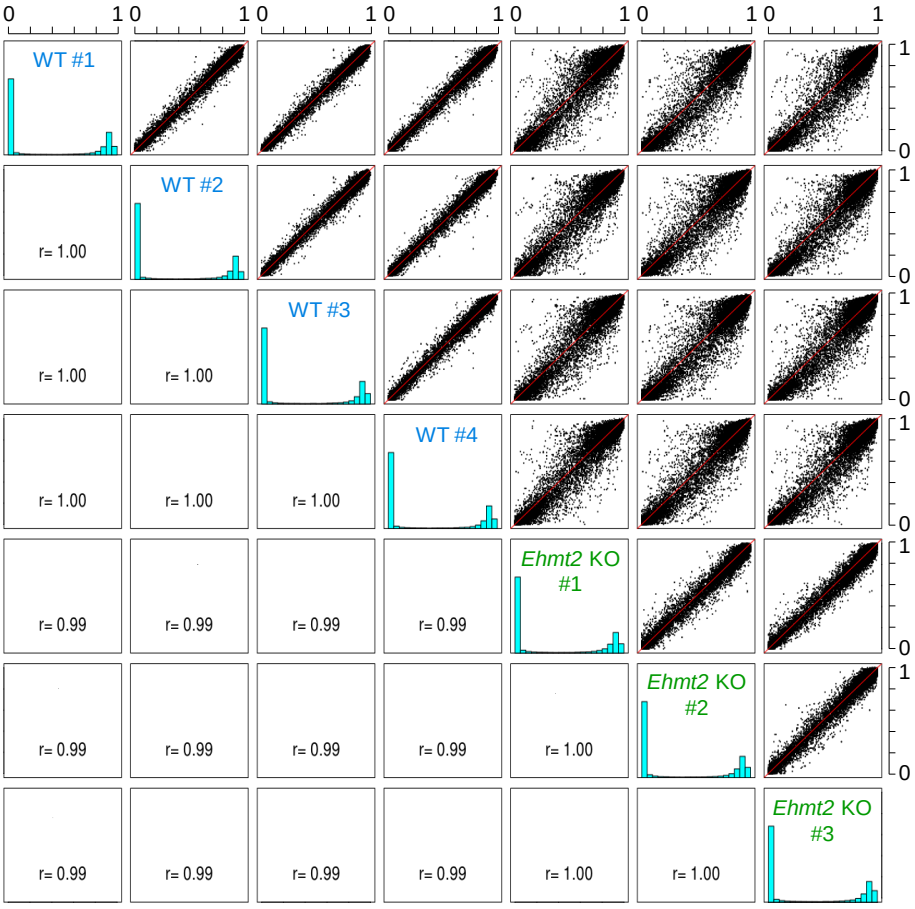

C

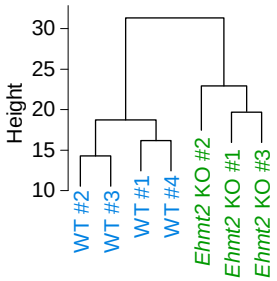

Supplemental Figure S3. Features of RRBS methylomes in WT and *Ehmt2*-/- embryos. A. Table summarizing the number of sequenced reads, mapped reads, the bisulfite conversion rate and the number of CpGs sequenced at least 8x. **B.** Correlation matrix of RRBS methylation scores between WT and *Ehmt2*-/- replicate embryos. The graphs show the correlation of methylation scores in 50,000 random genomic tiles (400bp) and the histograms show the distribution of methylation in all genomic tiles (400bp). The Pearson's correlation coefficients (r) are indicated. **C.** Dendrogram representing the hierarchical clustering of the RRBS methylation scores measured in genomic tiles (400bp).

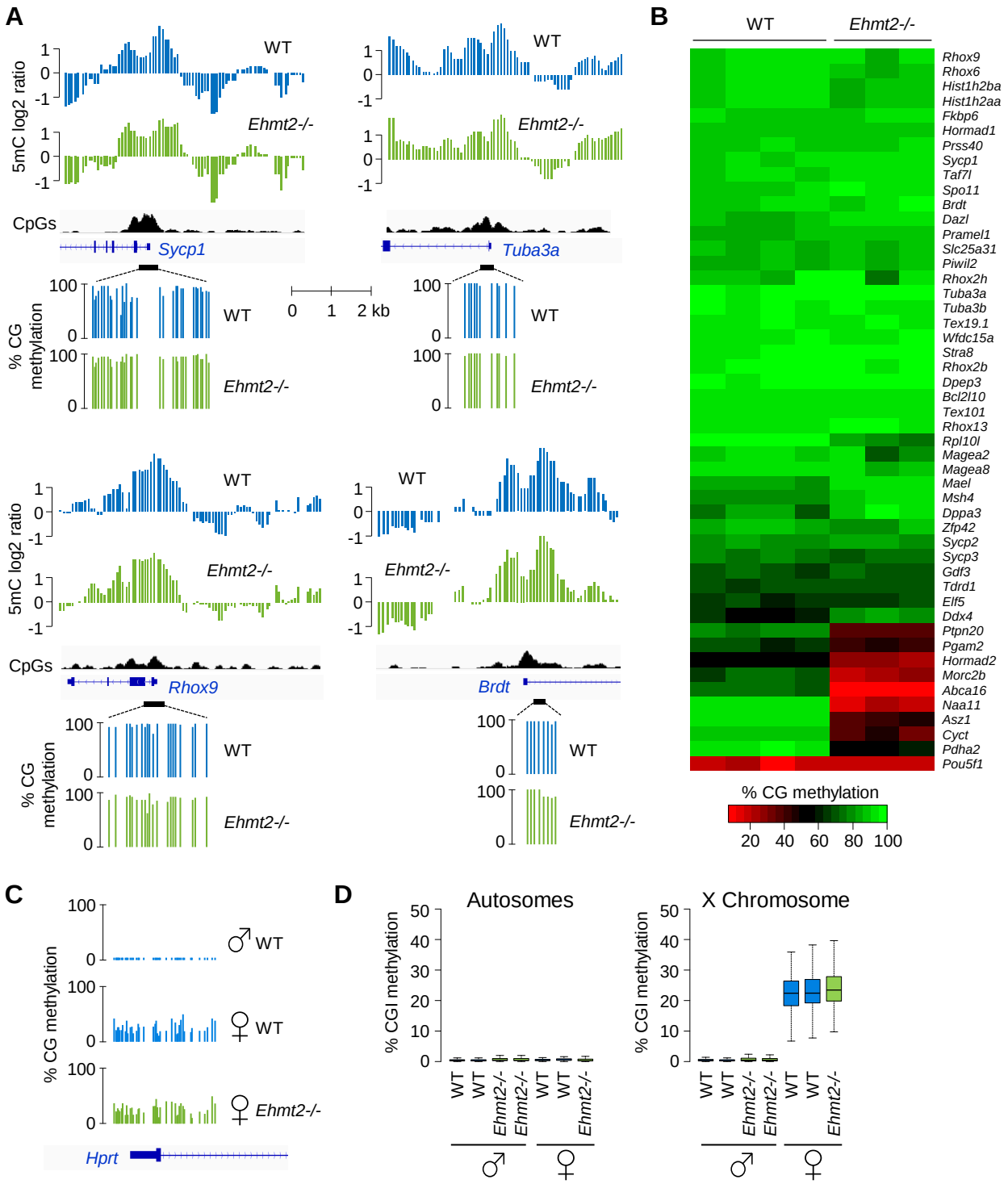

Supplemental Figure S4. Gene promoter methylation on autosomes and the X Chromosome in *Ehmt2-/-* embryos. A. MeDIP and RRBS profiles in the promoters of germline and placenta-specific genes. **B.** Heatmap representation of the RRBS methylation scores in gene promoters (-1000 to +1000 bp from the TSS) of germline and pluripotency genes. **C.** RRBS methylation scores in the CpG island promoter of the X-linked *Hprt* gene. **D.** Box plots of the methylation of autosomal and X-linked CpG islands in male and female embryos, indicating that EHMT2 is dispensable for CpG island methylation on the inactive X Chromosome in females.

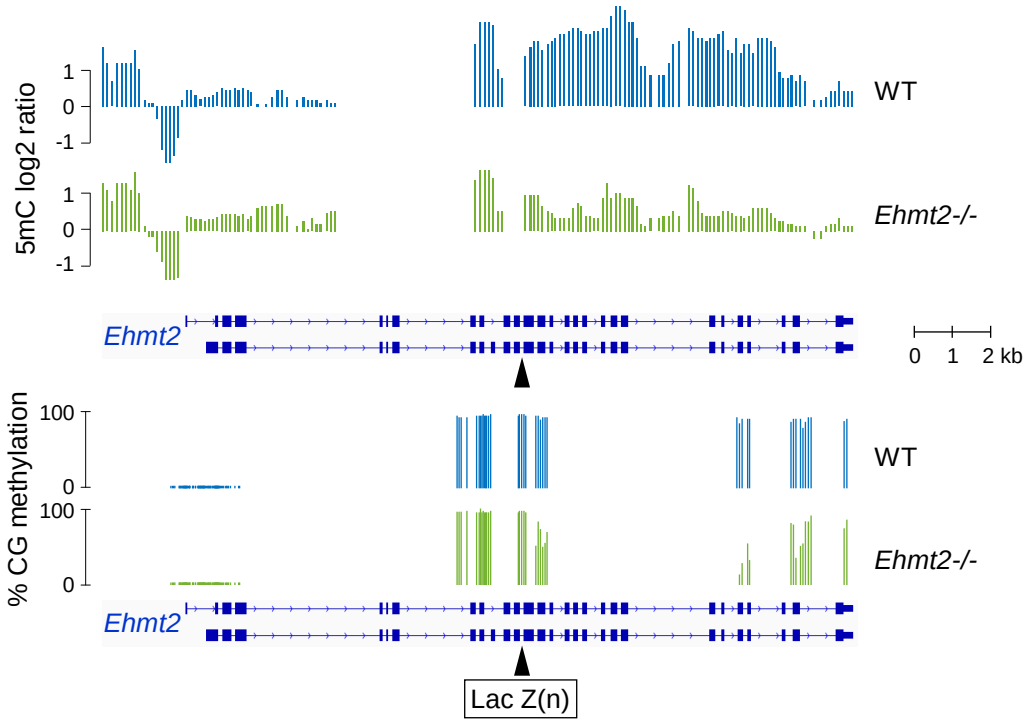

Supplemental Figure S5. Hypomethylation of the *Ehmt2* gene body in *Ehmt2-/-* embryos. The upper tracks depict smoothed MeDIP log2 ratios of individual oligonucleotides in the *Ehmt2* gene, and the graphs on the bottom depict methylation levels at individual CpGs covered by RRBS. The hypomethylation is detected by MeDIP and RRBS after the site of LacZ insertion (black arrow), beyond which transcription is aborted.

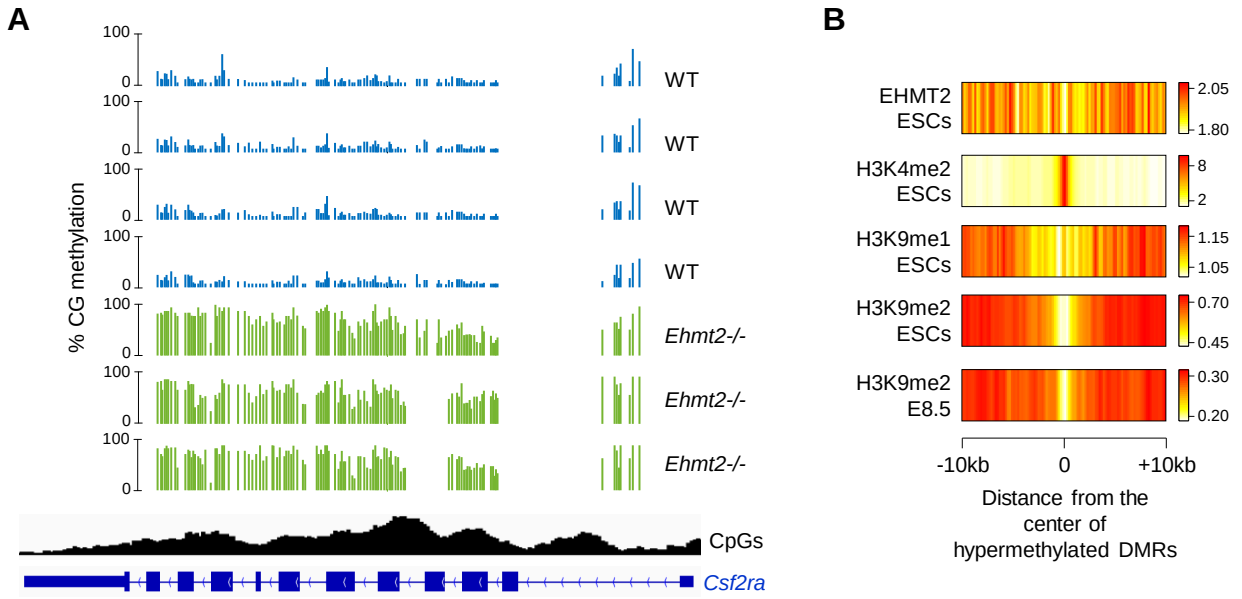

Supplemental Figure S6. Hypermethylated DMRs in *Ehmt2-/-* embryos. A. Example of hypermethylated DMR: a CpG island which covers the *Csf2ra* gene is hypermethylated in *Ehmt2-/-* compared to WT embryos. The graphs show RRBS methylation scores of individual CpGs in four WT and three *Ehmt2-/-* embryos. **B.** Heatmap representation of the distribution of EHMT2, H3K4me2, H3K9me1 and H3K9me2 at hypermethylated DMRs in mESCs and E8.5 embryos. The data represent the average density of ChIP-seq reads normalized by the density of reads in the input control.

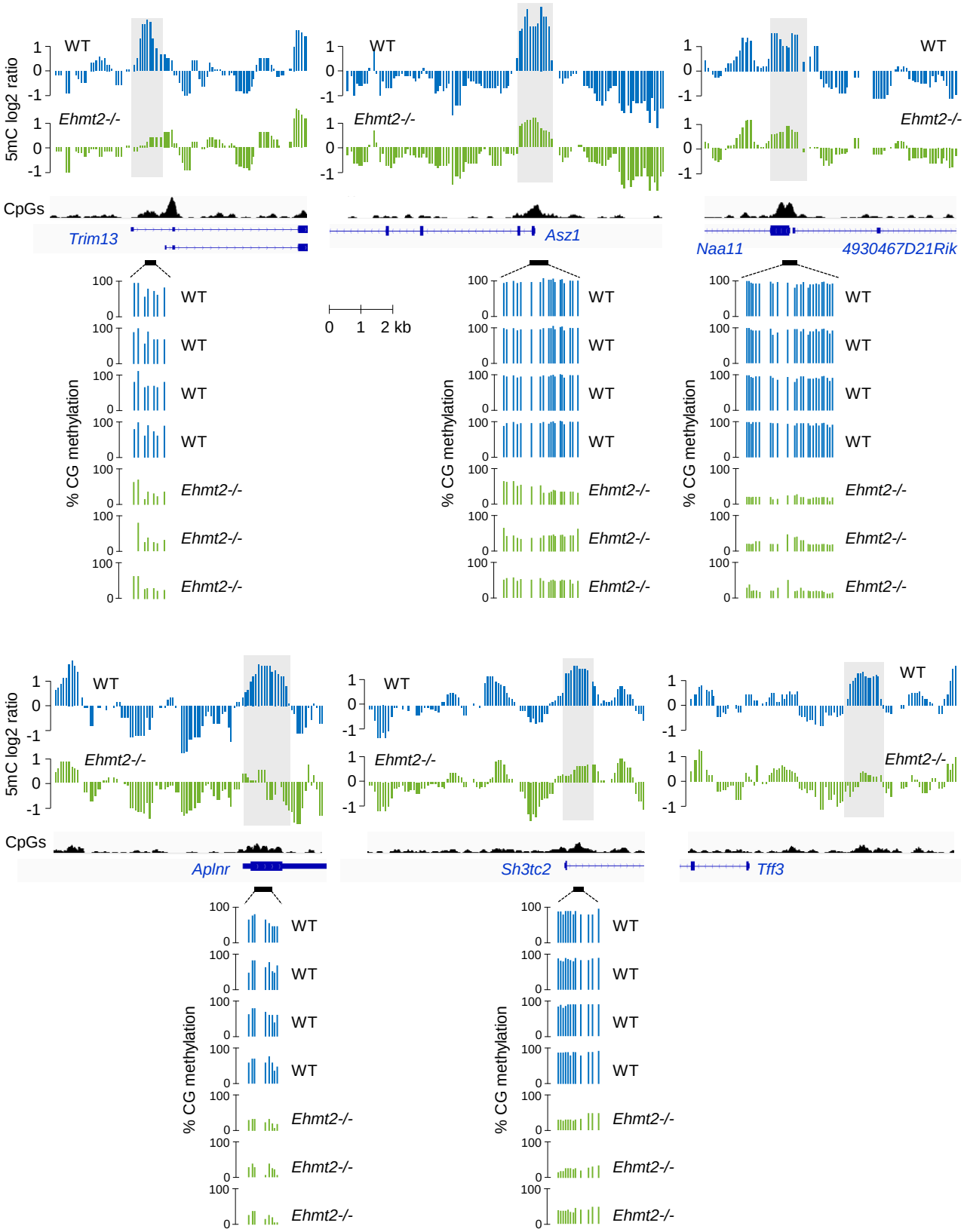

Supplemental Figure S7. Examples of hypomethylated regions (HMRs) in *Ehmt2-/-* embryos. The upper tracks depict smoothed MeDIP log2 ratios of individual oligonucleotides, and the graphs on the bottom depict RRBS methylation scores of individual CpGs in four WT and three *Ehmt2-/-* embryos. In each case, the difference measured by RRBS is confirmed by MeDIP (grey boxes).

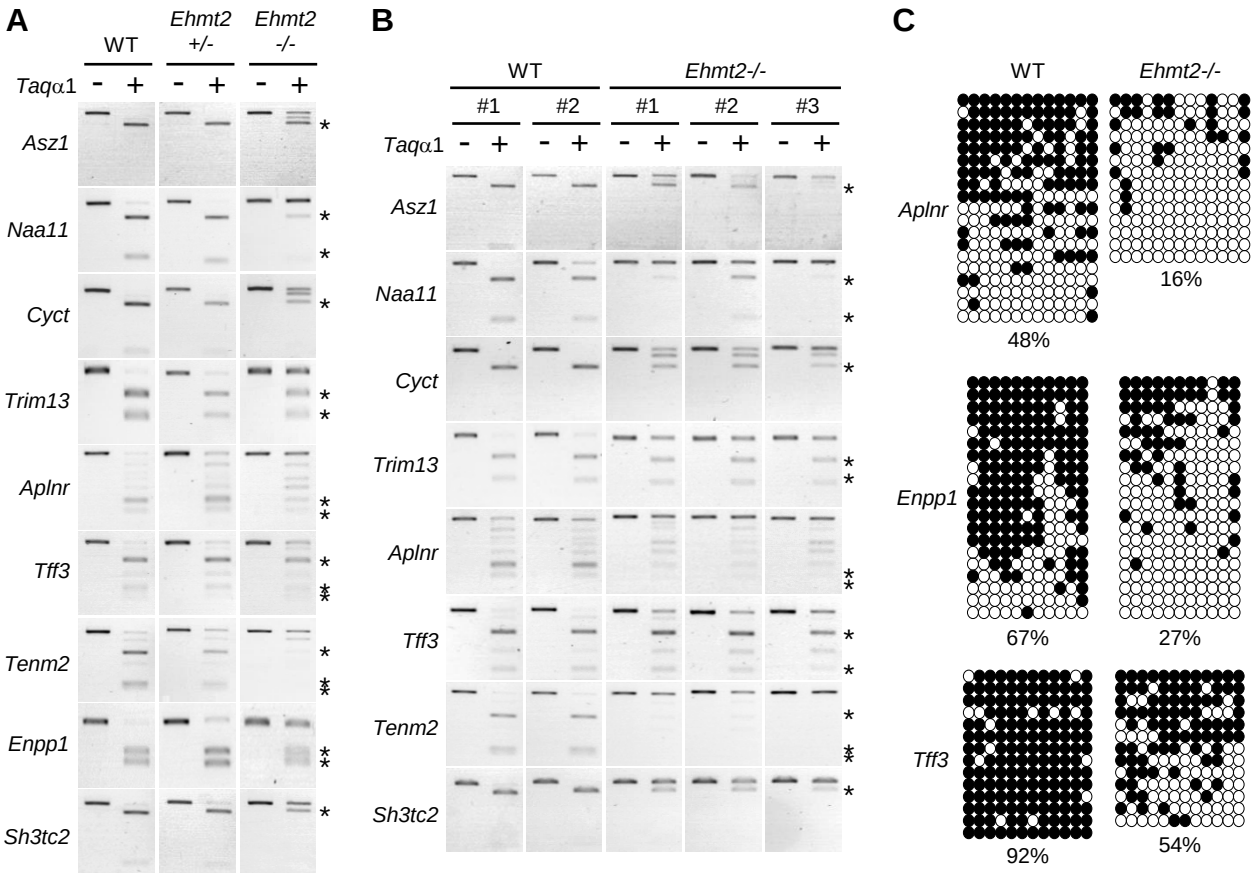

Supplemental Figure S8. Validations at sequences hypomethylated in *Ehmt2-/-* embryos. A. COBRA validations at candidate genes in wild type (WT), heterozygous (*Ehmt2+/-*) and homozygous mutant (*Ehmt2-/-*) littermate embryos collected at E9.5. The restriction fragments marked with asterisks are the end products of the digestion and indicate methylation. **B.** COBRA validations at eight target genes in two WT and three *Ehmt2-/-* embryos collected at E8.5. **C.** Bisulfite sequencing at three targets in WT and *Ehmt2-/-* E9.5 embryos. The percentages of CpG methylation per amplicon are indicated.

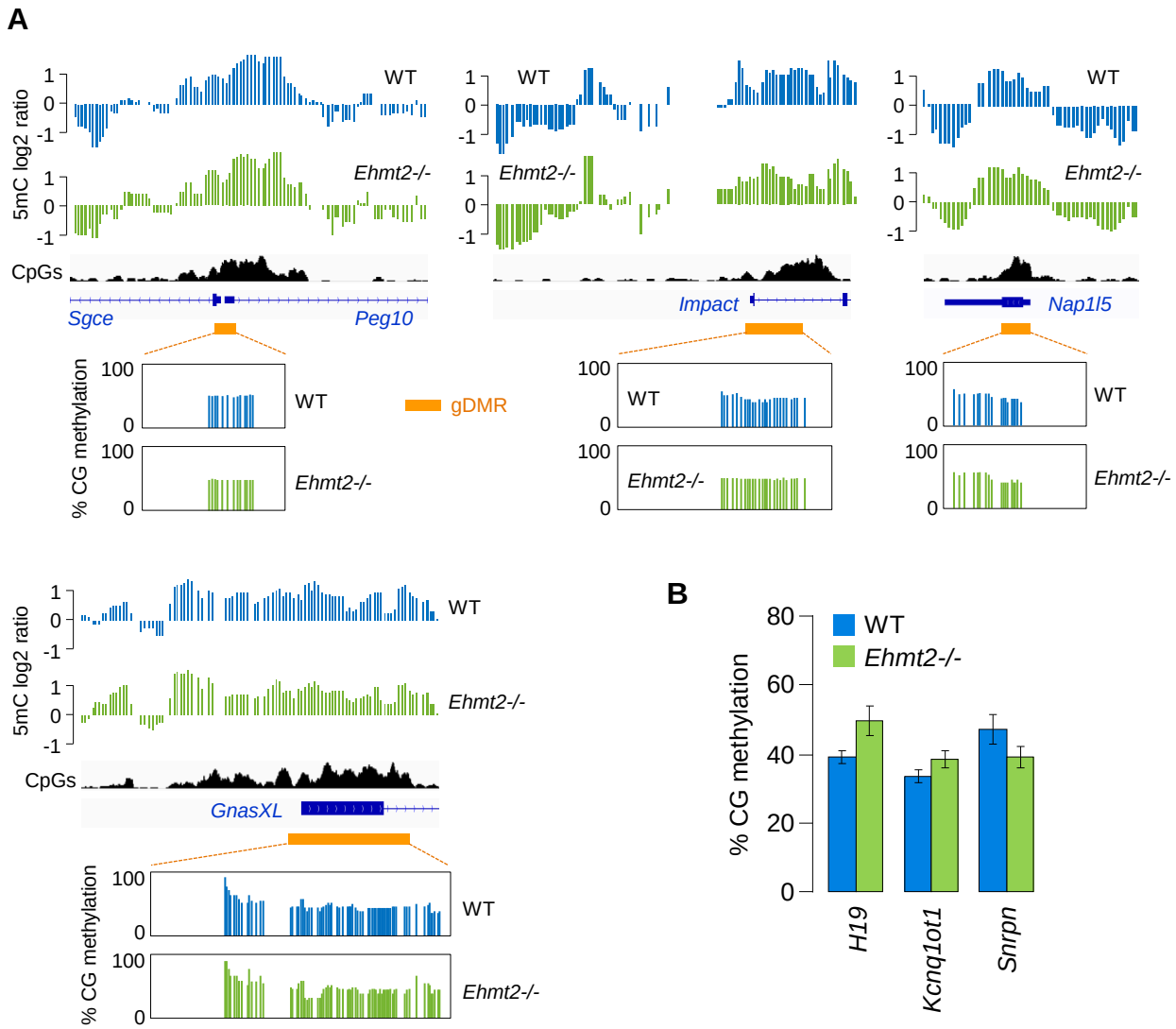

Supplemental Figure S9. DNA methylation of imprinted germline DMRs (gDMRs) in *Ehmt2-/-* embryos. A. Examples of DNA methylation profiles by MeDIP and RRBS at gDMRs. The orange bars mark the position of the gDMRs. **B.** Methylation analysis of three gDMRs by *Mcr*BC digestion followed by qPCR in E9.5 embryos (mean ± SD, n=3). Both paternal (*H19*) and maternal (*Kcnq1ot1*, *Snrpn*) gDMRs exhibit comparable methylation levels close to 50% in WT and *Ehmt2-/-* embryos.

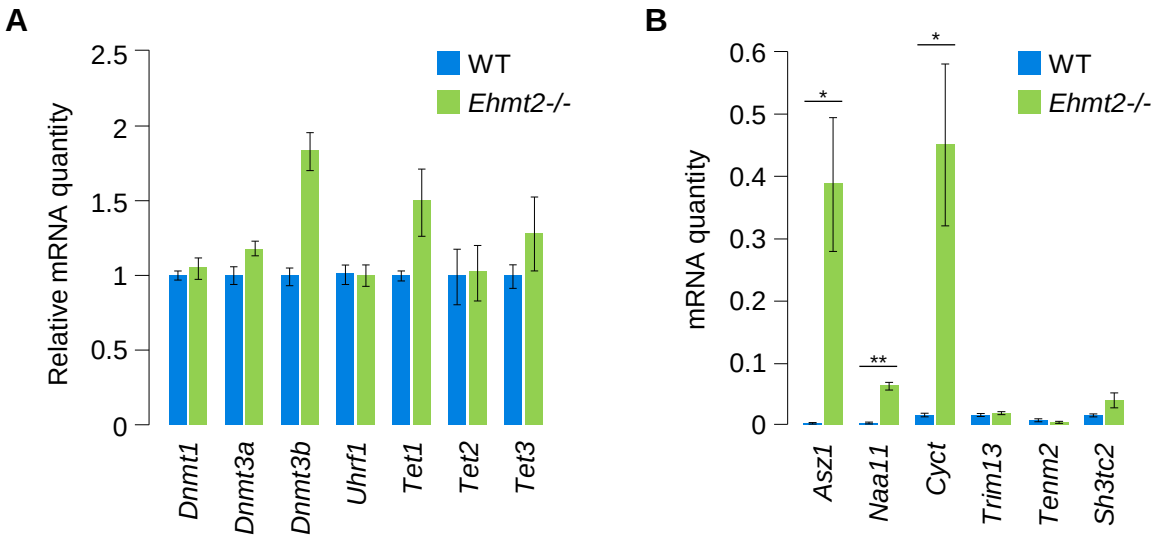

Supplemental Figure S10. Quantification of gene expression by RT-qPCR in *Ehmt2-/-* embryos. A. Expression of genes encoding components of the DNA methylation machinery in WT and *Ehmt2-/-* E9.5 embryos. Expression was normalized to the expression of two housekeeping genes (*Actb* and *Rpl13a*) and then the values in WT embryos were set at 1 (mean ± SEM, n=2 embryos). **B.** Expression of genes with a promoter-proximal HMR in WT and *Ehmt2-/-* E9.5 embryos, normalized to the expression of two housekeeping genes (*Actb* and *Rpl13a*) (mean ± SEM, n=3 embryos). * = $p<0.05$, ** = $p<0.01$ (t-test).

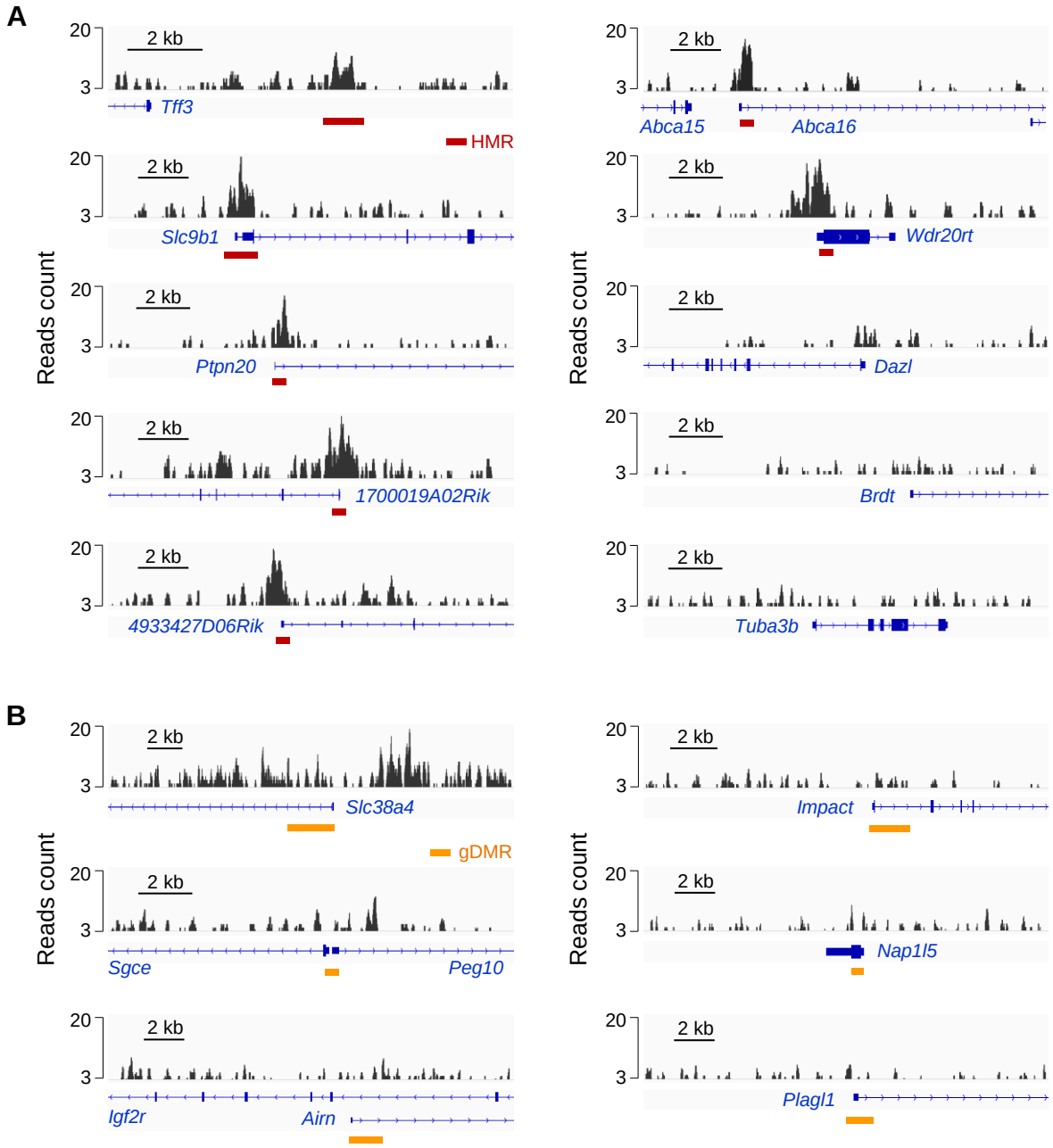

Supplemental Figure S11. EHMT2 ChIP-seq profiles in mESCs at promoter-proximal HMRs and imprinted gDMRs. A. Browser views of EHMT2 ChIP-seq profiles in WT TT2 m ESCs (Mozzetta et al., 2013) at several germline genes with reduced promoter DNA methylation in *Ehmt2-/-* embryos. In all cases, a peak of EHMT2 binding co-localizes with the HMR (red bars). In comparison, germline gene promoters with unchanged DNA methylation in *Ehmt2-/-* embryos (*Dazl*, *Brdt*, *Tuba3b*) are not enriched for EHMT2. **B.** EHMT2 ChIP-seq profiles in WT TT2 ESCs at imprinted gDMRs (orange bars). Enriched EHMT2 binding is detected in the vicinity of the *Slc38a4* gDMR but not at other gDMRs.

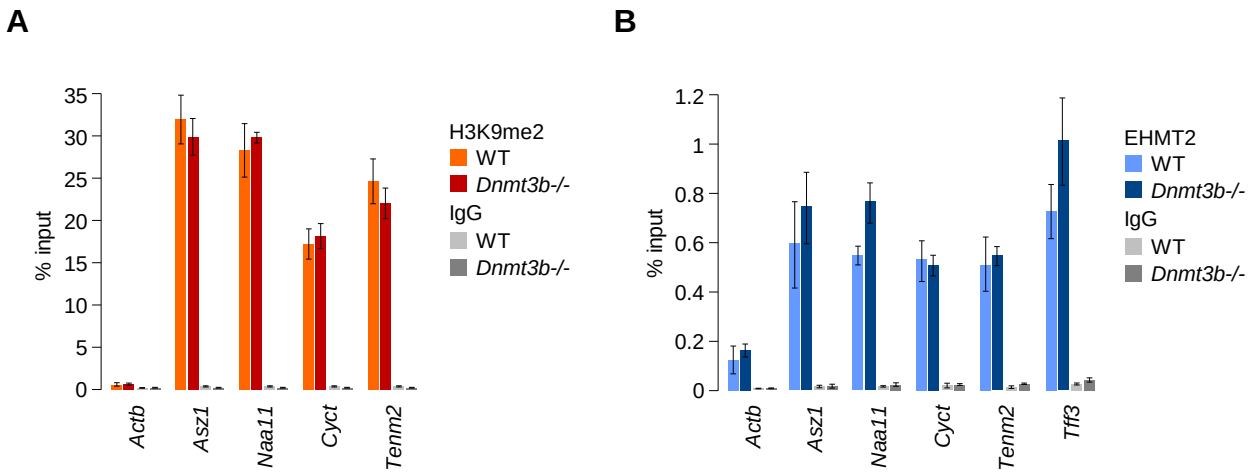

Supplemental Figure S12. ChIP-qPCR analysis of H3K9me2 and EHMT2 in WT and *Dnmt3b-/-* MEFs. A. ChIP-qPCR analysis of H3K9me2 at HMRs in primary MEFs derived from WT and *Dnmt3b-/-* embryos, represented as the percentage of input (mean ± SEM, n=4 for WT, n=3 for *Dnmt3b-/-*). The promoter of *Actb* served as a negative control. **B.** ChIP-qPCR analysis of EHMT2 binding at HMRs in primary MEFs derived from WT and *Dnmt3b-/-* embryos, represented as the percentage of input (mean ± SEM, n=2 for WT, n=4 for *Dnmt3b-/-*).

A

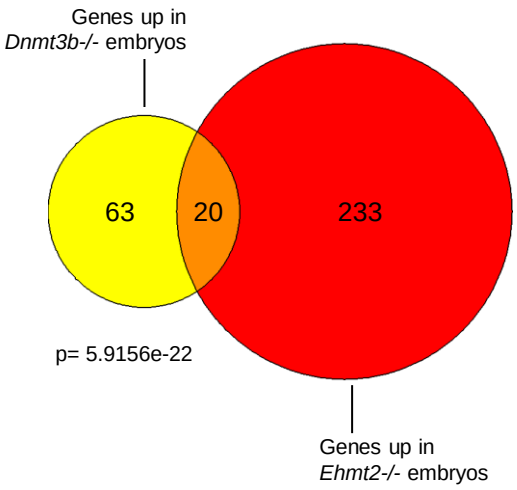

B

Up in *Dnmt3b-/-* and *Ehmt2-/-* embryos (n=20)

Asz1, Aurkc, Cyct, D1Pas1, Ddx4, Dppa4, Naa11, Nlrp4c, Psma8, Ptpn20, Rnf17, Rpl10l, Slc9b1, Sohlh2, Xlr, Xlr3a, Xlr3b, Xlr4a, Xlr4b, Xlr4c

Up in *Dnmt3b-/-* embryos only (n=63)

1300002E11Rik, 1700048O20Rik, 3830403N18Rik, A330102I10Rik, AU022751, Adad1, Bin2, Brdt, Ccdc152, Ccdc38, Dazl, Dppa3, EU599041, Fhit, Fkbp6, Gm13212, Gm14139, Gm1564, Gm7120, Gm9, Gpat2, Hist1h2aa, Hist1h2ba, Hormad1, Hsf2bp, Il2ra, Kbtbd12, Ly96, Mael, Mov10l1, Pabpc6, Papolb, Phf11d, Piwil2, Pou4f1, Ppp1r3fos, Rhox4e, Rhox4g, Rhox9, Rinl, Rpl39l, Slc25a31, Smc1b, Snora23, Snord111, Spaca1, Ssbp1, Stk31, Stra8, Syce1, Sycp1, Sycp2, Taf7l, Tdrd1, Tex11, Tex12, Topaz1, Tuba3a, Tuba3b, Usp26, Xlr3c, Zfp750, Zfp936

Up in *Ehmt2-/-* embryos only (n=233)

1700003M02Rik, 1700008I05Rik, 1700013H16Rik, 1700016K19Rik, 1700019E08Rik, 1700026D08Rik, 1700028P14Rik, 1700091H14Rik, 2410004P03Rik, 2410012E07Rik, 2610037D02Rik, 2610305D13Rik, 2900011O08Rik, 4430402I18Rik, 4922502N22Rik, 4930461G14Rik, 4930500J02Rik, 4930502E18Rik, 4930503E14Rik, 4930526L06Rik, 4933425L06Rik, 4933427D06Rik, 9430018G01Rik, A630023A22Rik, AA792892, AF067061, AI662270, Abca16, Acan, Ace, Ackr4, Acsbg1, Adgb, Aim2, Akr1c12, Ankrd66, Ano5, Aoah, Aqp8, Armc3, Atp2b2, Avpr1b, B020031M17Rik, BC080695, Btla, Btnl9, C330024D21Rik, C430002E04Rik, C8b, C920009B18Rik, Calb2, Camk1d, Capsl, Car3, Ccdc108, Ccdc146, Ccdc172, Cd3e, Cdx1, Ceacam20, Cer1, Cfap44, Cfap45, Cfap52, Cfc1, Cftr, Chrna9, Clca3, Cml5, Cox6b2, Cyp2b23, Cyp4f15, D630023F18Rik, Daw1, Dnah11, Dnah5, Dnah9, Dnajb13, Dnmt3l, Drc1, Dynlrb2, Efcab10, Elavl3, Enkur, Ephx2, Eras, Erich2, Fabp7, Fam183b, Fam212b, Fgf4, Fgf5, Foxh1, Foxi3, Foxj1, Gabre, Gal, Gca, Gfra3, Gm10451, Gm12794, Gm13051, Gm13078, Gm13119, Gm13154, Gm20767, Gm4841, Gm5622, Gm5771, Gm595, Gm6792, Gm773, Gm8267, Gm8994, Gmnc, Gna14, Gpx2, Grm8, Hist1h1t, Hormad2, Hydin, Igbp1b, Ina, Jade2, Kank4os, Khdc1a, Kifc2, Kndc1, LOC101056136, Lancl3, Ldhb, Lect2, Lincenc1, Lrrc10b, Lrrc48, Lrriq1, Lrriq4, Lrtm2, M1ap, Magea10, Magea2, Magea3, Magea4, Magea5, Magea8, Mcf2, Mesp1, Mfap5, Mlxipl, Mroh2b, Ms4a4d, Mup6, Myh3, Nckap1l, Neb, Nefm, Nme5, Nodal, Nxf3, Odf3b, Otof, Otog, Padi3, Pde1c, Pdha2, Pet2, Pgr, Phlda3, Pid1, Pifo, Pilrb2, Pim2, Plb1, Plekhd1, Pmaip1, Pou5f1, Pramef25, Ptk2b, Ptprq, Ptprtos, Rec114, Rhbg, Rhox2a, Rhox7a, Rlbp1, Rnase1, Rsph4a, Rxrg, Sct, Sh3gl3, Slc12a3, Slc19a2, Slc22a8, Slc27a2, Slc38a8, Slc47a2, Slc7a3, Spag17, Spata18, Spata31d1a, Spef2, Stat4, Syt4, Tcstv1, Tcstv3, Tdrd5, Tktl2, Tmem238, Tmem92, Toporsl, Tph2, Trh, Trim13, Trp53inp1, Trp73, Tsga8, Ttc39b, Ubxn10, Usp17le, Utf1, Vrtn, Vwa3a, Wdr63, Wnt8a, Xlr5a, Xlr5b, Xlr5c, Zfp36l3, Zic3, Zmat4, Zscan4b, Zscan4d, Zscan4f

Supplemental Figure S13. Comparison of genes upregulated in *Ehmt2-/-* and *Dnmt3b-/-* E8.5 embryos. A. Venn diagram showing the overlap between the genes upregulated in *Ehmt2-/-* and *Dnmt3b-/-* E8.5 embryos (Auclair et al. 2014). We defined upregulated genes as having a fold change greater than 3 and an adjusted p value below 0.01. The p value below the Venn diagram indicates the significance of the overlap (hypergeometric test). **B.** Lists of genes upregulated at least 3-fold in both KO lines or exclusively in one KO line.